

## DESIGN OF MODIFIED 6–18 GHz BALANCED ANTIPODAL VIVALDI ANTENNA

P. Wang<sup>1,3,\*</sup>, H. Zhang<sup>2</sup>, G. Wen<sup>1</sup>, and Y. Sun<sup>1</sup>

<sup>1</sup>Centre for RFIC and System Technology, School of Communication and Information Engineering, University of Electronic Science and Technology, Chengdu 611731, China

<sup>2</sup>Science and Technology on Electronic Information Control Laboratory, Chengdu 610036, China

<sup>3</sup>College of Electronic and Information Engineering, Chongqing Three Gorges University, Chongqing 404000, China

**Abstract**—In this paper, a modified planar balanced Vivaldi antenna with endfire characteristics near the metal surface is proposed for 6–18 GHz applications. The proposed antenna structure consists of three copper layers, among which two external layers locate on the two outsides of two dielectric substrates, and the central layer is sandwiched by these two dielectric substrates. To further enhance the end-fire radiation characteristic, a number of novel techniques are proposed, including elongation and shaping of the supporting substrate of a conventional balanced antipodal Vivaldi antenna beyond its aperture, using an I-shaped slot loaded radiation patch and cutting a triangle on the edge of three copper layers. Measured and simulated results show that the proposed antenna not only exhibits good impedance bandwidth, but also improves the end-fire performance in the operational frequency of 6–10 GHz and achieves high gain in the end-fire direction, low cross-polarization and high front-to-back (F-to-B) ratio.

---

*Received 12 October 2011, Accepted 30 November 2011, Scheduled 4 December 2011*

\* Corresponding author: Ping Wang (wangpingcqz@163.com).

## 1. INTRODUCTION

Since Gibson presented the new structure of slotline antenna based on an exponentially tapered flare and described it as a class of frequency-independent radiators, called as conventional Vivaldi tapered slot antennas [1], many literatures [2–10] have studied this type of antenna element. A few of investigations of single antenna with different shapes of the tapered slot were found in [2–5], including exponentially tapered slot, logarithmically tapered slot antenna (TSA), linearly tapered slot and constant width slot, which gave many empirical equations. Ref. [6] investigated how different outer edge taper parameters affected the far-field performance, which shows that dual exponentially tapered slot antenna (DE TSA) has excellent performance compared to an exponentially tapered slot antenna, such as higher directivity, narrower beamwidth, shorter size and lower cross polarization level. Both co- and cross-polarization radiated fields were discussed in [7] by using dyadic Green's functions. However, the bandwidth of the conventional Vivaldi tapered slot antenna is limited by the transition between the feed and the antenna slot [11, 12]. Previously, Gazit [13] introduced the antipodal Vivaldi antenna, which exhibits broadband characteristic. Subsequently, many researchers have explored its performance, including further enhancement of the bandwidth [14], dispersion behavior of two specific Vivaldi antennas in both frequency and time domains [15], Vivaldi antenna arrays for see through dry wall and concrete wall UWB applications [16], miniaturization of antenna [17–19]. However, the antipodal nature of the antenna gives rise to not only very high levels of cross-polarization, but also severe polarization tilt as the frequency of operation is increased. To overcome these problems, by adding another dielectric layer and an extra layer of metallization, the electric field in the slot region is oriented parallel to the metallization, namely balanced antipodal Vivaldi antenna is formed, which has smaller cross-polarization level of  $-15$  dB for 6 GHz–18 GHz [11, 12]. Recently, several approaches have been suggested in improving end-fire radiation pattern of balanced Vivaldi antenna, i.e., introducing a dielectric director in radiation aperture [20, 21]. A novel technique of elongating and shaping of the supporting substrate of a conventional balanced antipodal Vivaldi antenna beyond its aperture is introduced [22]. Tapered slot antenna is embedded in a dielectric rod [23], which obtains good performances such as wide operating bandwidth, low cross-polarization, higher gain, smaller tilt angle of its main beam, improvement of the Vivaldi phase center variation.

In this paper, we propose a simple balanced Vivaldi antenna near a metallic surface, which presents excellent end-fire features

by prorogating the supporting substrate of a conventional balanced antipodal Vivaldi antenna and changing the shape of substrate and radiation patch. Simulated and experimental results demonstrate that the proposed antenna has wide operating bandwidth, low cross-polarization, high front-to-back (F-to-B) ratio, and high gain.

## 2. ANTENNA GEOMETRY

Figure 1 illustrates the geometry and detailed parameters of the proposed antenna. The conventional balanced Vivaldi antenna (CBVA) is shown in Fig. 1(a), which adopts a novel technique of elongating and shaping of the supporting substrate of an original balanced antipodal Vivaldi antenna beyond its aperture used in [22].

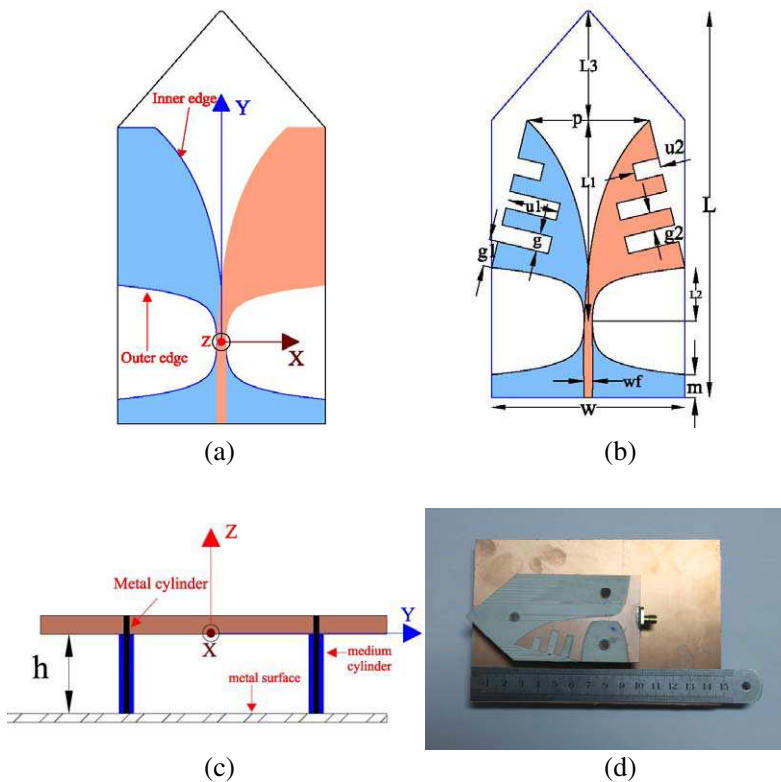


**Figure 1.** (a) Conventional balanced Vivaldi antenna (CBVA). (b) Modified balanced Vivaldi antenna (MBVA). (c) Modified balanced Vivaldi antenna near a metal surface. (d) Prototype of the proposed antenna.

It consists of three copper layers, the two external layers locating in the exterior of two dielectric substrates and two dielectric substrates sandwiching the central layer. This layout constrains electric field in the slot region parallel to the metallization, aiming to improve the cross-polarization level. The exponential profile curves of inner and outer edge employed in this design can be described by the equation

$$\begin{aligned} x_i &= \pm 0.5 \times wf \pm 0.5 \times w1 \times \exp(k_s y) \mp 0.5 \times w1 \\ x_o &= \pm 0.5 \times wf \pm 0.5 \times w2 \times \exp(k_w y \wedge sf) \mp 0.5 \times w2 \end{aligned} \quad (1)$$

where  $x_i$  and  $x_o$  denote the distances from the slot center line to the inner and outer edges, respectively. The quantity  $wf$  is the total strip-feed width, and  $k_s$  specifies how the slot widens as the distance from the slot center line to the inner edge is increased.  $k_w$  determines the side intercept for outer edge taper curves. The coefficient  $sf$  determines the shape of the outer edge taper. The quantity  $w1$  and  $w2$  also adjust the shape of dual exponentially tapered cures. Fig. 1(b) shows the modified balanced Vivaldi antenna (MBVA), which only cuts triangular patch along the terminal of two dual exponential curves and loads three I-shaped notched slots on the edge of every copper layer. With this modification, the radiation pattern of the proposed antenna is further improved, especially in the lowest frequency band (6 GHz–10 GHz). The modified antenna has a size of  $50.06(W) \times 101(L)$  mm<sup>2</sup> and is constructed using Rogers RO4003 (thickness = 1.5 mm, dielectric constant = 3.38 and loss tangent 0.0027). Fig. 1(c) shows the proposed antenna when placed close to the metallic surface with a distance  $h$ . The proposed structure is optimized using Ansoft's high frequency structure simulator (HFSS 10), which utilizes the finite element method for electromagnetic simulation. A  $50 \Omega$  SMA connector serves as the antenna port.

### 3. ANALYSIS AND EXPERIMENTAL RESULTS

#### 3.1. Slot-loaded and Triangle-cut Vivaldi Antenna

To achieve high front-to-back ratio, the slot-loaded and triangle-cut balanced Vivaldi antenna is proposed in Fig. 1(b). By fine tuning and optimization, the final optimal dimensions are obtained and eventually determined with  $w1 = 1.7304$  mm,  $w2 = 0.18$  mm,  $L1 = 52.5$  mm,  $L2 = 14$  mm,  $L3 = 28.5$  mm,  $wf = 2.1$  mm,  $m = 6$  mm,  $u_1 = 13.5$  mm,  $u_2 = 7$  mm,  $g = 4.5$  mm,  $g1 = 7$  mm,  $g2 = 4.5$  mm,  $h = 10$  mm,  $p = 32$  mm,  $ks = \ln((wf + p + w1)/w1)/L1$ ,  $kw = 0.4$ ,  $sf = 1$ . A fabricated antenna is tested using an Agilent N5230A series vector network analyzer. Fig. 2 shows the simulated and measured reflection coefficients against frequency. It is observed that

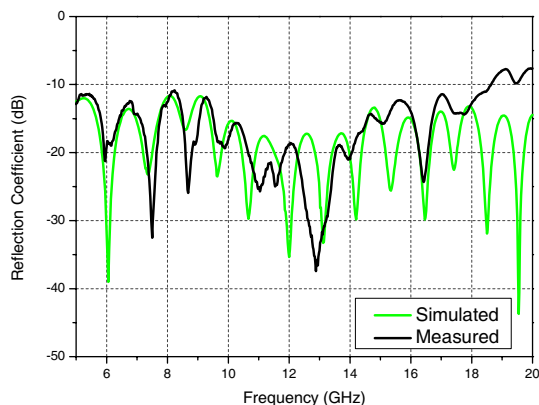


**Figure 2.** Simulation and measured reflection coefficient for the proposed antenna.

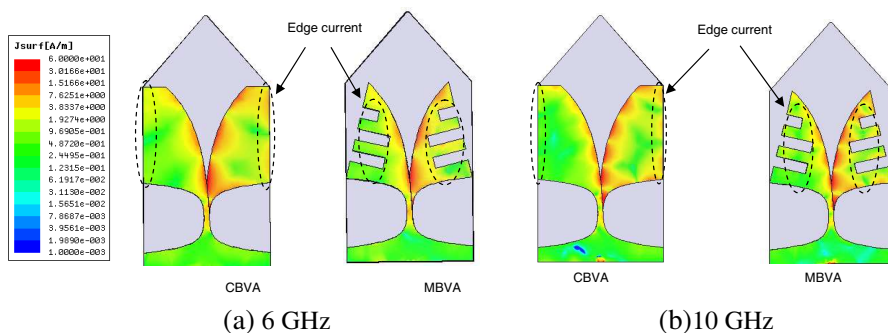
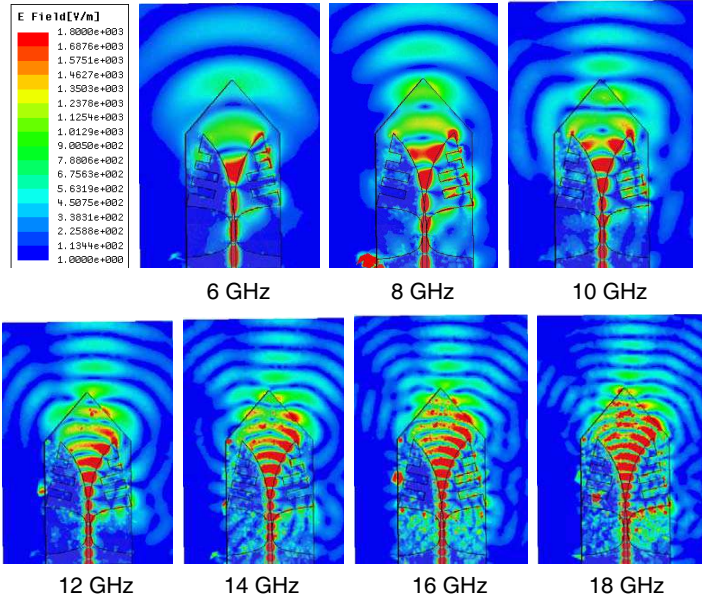


**Figure 3.** Surface current distribution for both CBVA and MBVA at 6 GHz and 10 GHz, respectively.

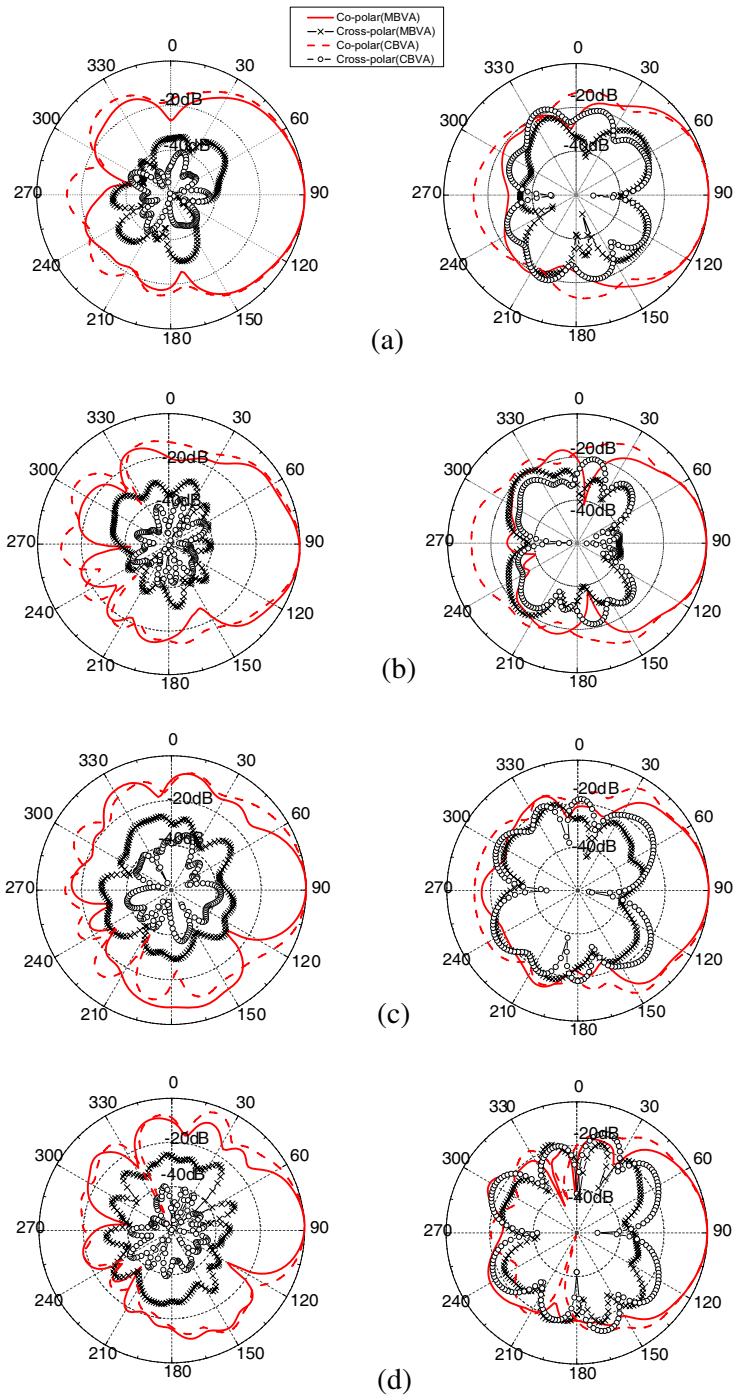
a good agreement between the simulation and measurement results is achieved, and the proposed antenna has a very good bandwidth for 6–18 GHz applications. A minor discrepancy is also observed owing to the following possible effect factors: 1) the joining of the SMA connector (solder roughness), 2) the indoor measurement environment, 3) imperfections in manufacturing, 4) calibration error of network analyzer at higher frequency.

With the help of the simulator HFSS, the surface current distribution of both conventional balanced Vivaldi antenna (CBVA) and modified balanced Vivaldi antenna (MBVA) can be studied at 6 GHz and 10 GHz, which is presented in Fig. 3. As shown in black-dash-line region, the conventional balanced Vivaldi antenna has

strong edge current, which radiates vertically with end fire direction. However, by etching I-shaped slots and cutting triangle on radiation patch, significant currents paths in black-dash-line region have been altered as shown in Fig. 3. The behaviors not only reduce the quality factor  $Q$  of the antenna and extend the lower end bandwidth, but also enhance the endfire direction radiation and weaken the back-direction radiation, so excellent end-fire features may be achieved. Nevertheless, because of frequency-independent characteristic of Vivaldi antenna, the wideband character and miniaturization of the Vivaldi antenna are not our main aims in this paper. We will keep a large size of antenna to achieve high gain, and pay more attention to high gain and front-to-back ratio of the antenna. The simulated  $E$ -field distributions are depicted in Fig. 4 for 6 GHz, 8 GHz, 10 GHz, 12 GHz, 14 GHz, 16 GHz and 18 GHz on  $xy$ -plane, respectively, which spread along the slot region and are guided by the triangular dielectric substrate. The generated electric field radiates at the top edge of the antenna. It is observed obviously that the proposed antenna has strong endfire radiation character in the whole working frequency band. Its main beam has very small tilt in high frequency band, and grating lobes appear as the frequency increases.



**Figure 4.** Simulated  $E$ -field at 6 GHz, 8 GHz, 10 GHz, 12 GHz, 14 GHz, 16 GHz and 18 GHz on  $xy$ -plane.



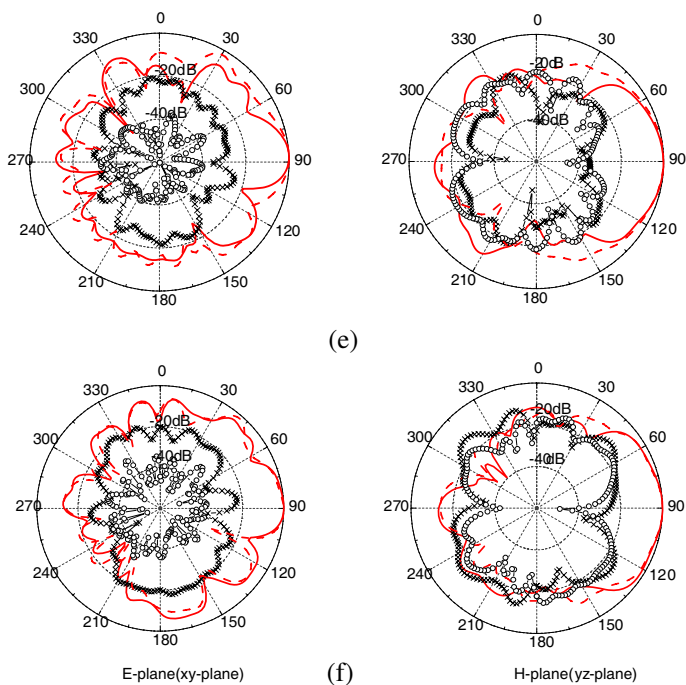


**Figure 5.** Simulated radiation patterns for both conventional balanced Vivaldi antenna (CBVA) and modified balanced Vivaldi antenna (MBVA) at (a) 6 GHz, (b) 8 GHz, (c) 10 GHz, (d) 12 GHz, (e) 14 GHz, (f) 16 GHz.

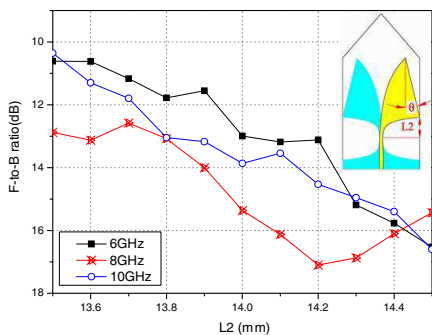


**Figure 6.** Simulated F-to-B ratio for the proposed antenna as a function of  $L_2$ .

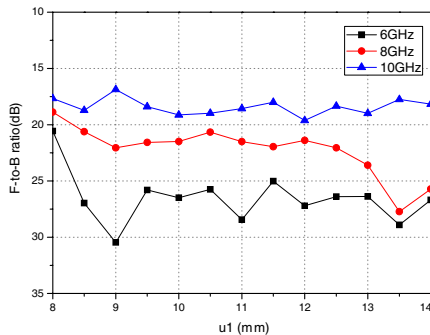


**Figure 7.** Simulated F-to-B ratio for the proposed antenna as a function of  $u_1$ .



To show the improved performance, Fig. 5 plots the simulated far-field radiation patterns of both conventional balanced Vivaldi antenna(CBVA) and modified balanced Vivaldi antenna(MBVA) for  $E$ -plane ( $xy$ -plane) and  $H$ -plane ( $yz$ -plane). Here two antennas keep same parameters. It is seen that the modified balanced Vivaldi antenna has good end-fire performance with the main lobe pointing in the axial direction of the tapered slot ( $y$  direction in Fig. 1), namely maximal electric field is located in the  $y$ -direction. Compared to the conventional balanced Vivaldi antenna, the proposed antenna has higher front-to-back ratio at 6–10 GHz, and the radiation pattern has little change in higher frequency. The modification also results in larger cross-polarization in  $E$ -plane. It is also observed that all the operating frequencies have the same polarization plane and similar radiation patterns throughout the entire range of frequencies, and the  $H$ -plane pattern shows relatively large cross-polarization compared with the  $E$ -plane pattern. This behavior is largely due to the strong horizontal components of the surface current and electric field because the vertical component of the surface current is the main contributor to the radiation and because the horizontal component contributes to the cross-polarization.

Figure 6 presents the effect of  $L_2$  variation on the F-to-B ratio only at 6 GHz, 8 GHz and 10 GHz. It is seen that the effect of  $L_2$  on the F-to-B ratio is same with that of the quantity  $\theta$ , and when the quantity  $L_2$  increases, the F-to-B ratio of the antenna is improved. However, the behavior of increasing  $L_2$  will increase the width of the antenna, which does not meet the requirement of small size in width. In the design of the antenna, the quantity  $L_2$  is selected as 14 mm. When the length  $u_1$  of the I-shaped notched slot is changed with the

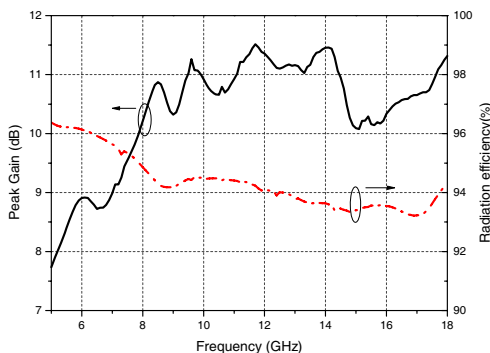


**Figure 8.** Simulated peak realized gain and radiation efficiency of the modified balanced Vivaldi antenna.

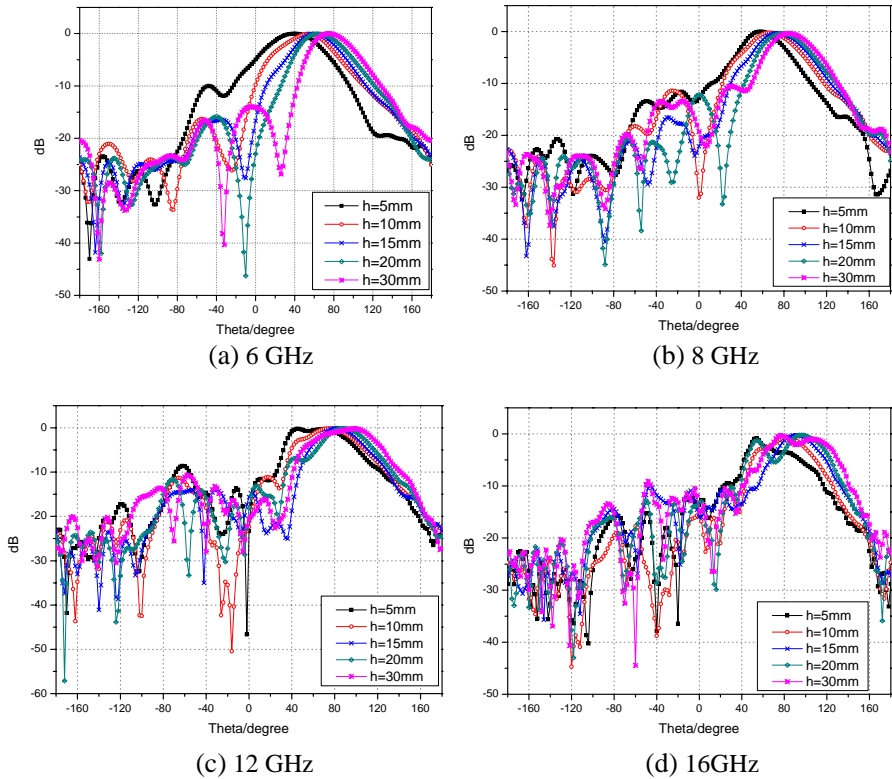


**Figure 9.** Simulated co-polar radiation patterns (in  $H$ -plane) of the modified balanced Vivaldi antenna near a metallic surface as a function of  $h$ , the distance between the proposed antenna and metallic surface.

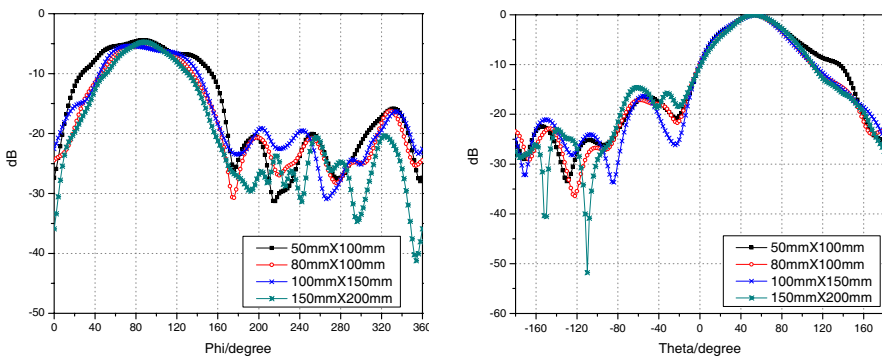
other parameters fixed, Fig. 7 presents the simulated F-to-B ratio for different values of  $u_1$ . As the figure describes, the three curves have a little change. Nevertheless, by the comparison of Fig. 7 and Fig. 6, the F-to-B ratio can be further improved, which indicates that the I-shaped notched slot affects the performance of the F-to-B ratio, especially in lower frequency.

Figure 8 shows the simulated peak realized gains and radiation efficiency across the whole operating frequency bands. It is observed that the peak gain of the antenna varies from 8.7 dB to 11.5 dB, that the maximum value is about 11.5 dB at 11.7 GHz, and that the radiation efficiency is stable, which varies around 94% for the operating band of 6–18 GHz. The high radiation efficiency may have low loss in Rogers RO4003 substrate (a loss tangent of 0.0027), which results in high gain and radiation efficiency in the whole frequency band. As a result, the

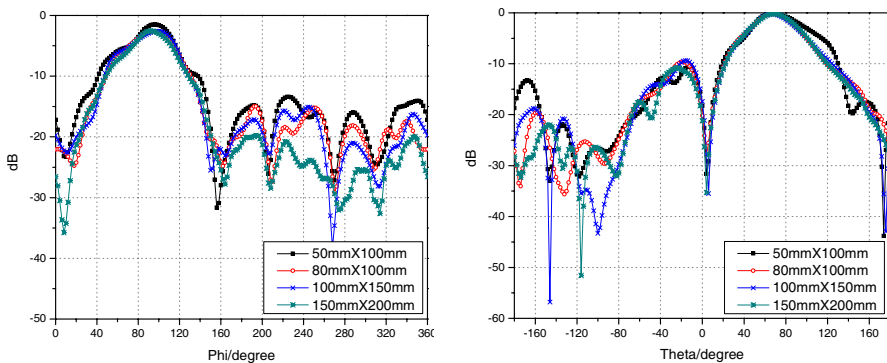
gains of the proposed antenna within the operating band are enough to meet the engineering requirement.

### 3.2. Modified Balanced Vivaldi Antenna Near a Metallic Surface

The modified balanced Vivaldi antenna is placed above a ground plane ( $W_{gr} \times L_{gr}$ ) at a height of  $h$ . As shown in Fig. 1(c), the triangular substrate's top side is parallel to the short edge of the metal surface, and the antenna is supported by using three metal cylinders with radius of 0.6 mm, and three substrate cylinders with relative permittivity of 2.1, tangent loss of 0.00045 and radius of 1.2 mm. Fig. 9 shows the effects of the distance  $h$  between the proposed antenna and metallic surface on far-field co-polar radiation patterns (in  $H$ -plane), where the ground plane is a rectangular patch with dimensions of 100 mm  $\times$  150 mm ( $W_{gr}$ )  $\times$  150 mm ( $L_{gr}$ ) and the other parameters of the proposed



(a) 6 GHz



(b) 8 GHz

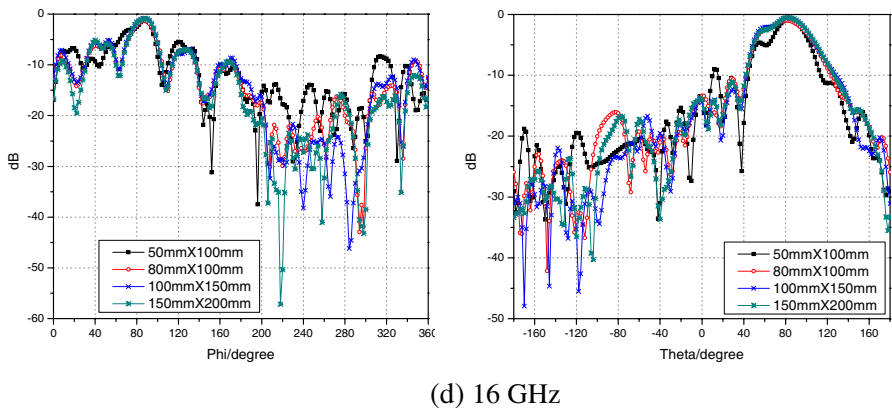
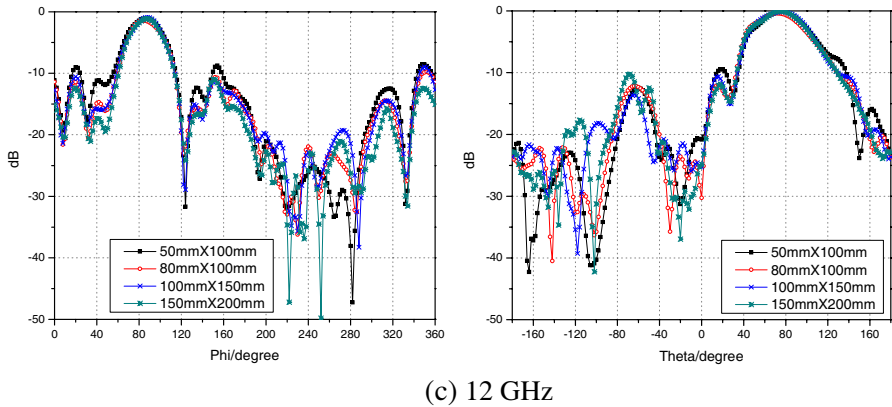


**Figure 10.** The effect of the size of ground plane on radiation patterns at (a) 6 GHz, (b) 8 GHz, (c) 12 GHz, (d) 16 GHz.

antenna keep invariable. As shown in Fig. 9, when the distance  $h$  varies from 5 mm to 30 mm, the main lobe has a little tilted angle away from endfire direction ( $y$ -direction) due to the reflection from the metal surface, and maximal value happens in 6 GHz. When the distance  $h$  is 10 mm, the maximal angle is about 30 degree. It is also observed carefully that the tilted angle decreases slightly with the increase of frequency.

Figure 10 shows the effect of the size of the ground plane on far-field radiation pattern for  $E$ -plane ( $xy$ -plane) and  $H$ -plane ( $yz$ -plane). It is observed that the radiation pattern is affected slightly. When the size of ground plane increases, the beamwidth of the co-polarization radiation pattern becomes narrower in  $E$ -plane and is nearly invariable

in  $H$ -plane, with the main beam direction nearly motionless. In this part, we discuss the performance of the proposed antenna near metallic surface, which proves that the antenna can be located on metallic surface of a variety of aerocrafts, such as missile.

#### 4. CONCLUSION

In this paper, a modified balanced Vivaldi antenna has been proposed for 6–18 GHz applications. The proposed antenna can achieve good impedance bandwidth, good end-fire radiation performance, high gain in the end-fire direction, low cross-polarization and high F-to-B ratio through loading I-shaped notched slots and cutting a triangle on the edge of three copper layers. Compared to conventional balanced Vivaldi antenna in [22], the proposed antenna has smaller size and higher front-to-back ratio at 6–10 GHz. In addition, we have also presented the radiation pattern of the proposed antenna near a metal surface and fabricated a prototype of the proposed antenna. It is found that the radiation pattern is affected slightly in the  $E$ -plane, whereas the main beam direction of the co-polarization radiation pattern is tilted toward the axial direction with a small angle due to the reflection of the metal surface in the  $H$ -plane. Therefore, the proposed antenna can be an excellent candidate for satellite communication systems and a variety of advanced aircraft systems.

#### ACKNOWLEDGMENT

This work is supported by a Major Project of Science and Technology on Electronic Information Central Laboratory of China under Grant No. M16010101SYSJJ2010-5.

#### REFERENCES

1. Gibson, P. J., "The Vivaldi aerial," *9th Eur. Microw. Conf.*, 101–105, Brighton, UK, 1979.
2. Yngvesson, K. S., D. H. Schaubert, T. L. Korzeniowski, E. L. Kollberg, and T. Thungren, "Endfire tapered slot antennas on dielectric substrates," *IEEE Trans. Antennas Propag.*, Vol. 33, 1392–1400, 1985.
3. Wang, N. B., Y. C. Jiao, Y. Song, L. Zhang, and F.-S. Zhang, "A microstrip-fed logarithmically tapered slot antenna for wideband applications," *Journal of Electromagnetic Waves and Applications*, Vol. 23, No. 10, 1335–1344, 2009.

4. Wang, N. B., Y. Song, Y. C. Jiao, L. Zhang, and F.-S. Zhang, "Extreme wideband tapered slot antenna with impedance bandwidth in excess of 21.6:1," *Journal of Electromagnetic Waves and Applications*, Vol. 23, No. 2–3, 231–238, 2009.
5. Hu, S., C. L. Law, and W. B. Dou, "A tapered slot antenna with flat and high gain for ultra-wideband applications," *Journal of Electromagnetic Waves and Applications*, Vol. 23, No. 5–6, 723–728, 2009.
6. Greenberg, M. C., K. L. Virga, and C. L. Hammond, "Performance characteristics of the dual exponentially tapered slot antenna for wireless communications applications," *IEEE Trans. Vehicular Tech.*, Vol. 52, No. 2, 305–312, Mar. 2003.
7. Stockbroeckx, B. and A. V. Vorst, "Copolar and cross-polar radiation of Vivaldi antenna on dielectric substrate," *IEEE Trans. Antennas Propag.*, Vol. 48, 19–25, 2000.
8. Atiah, A. and N. Bowring, "Design of flat gain UWB tapered slot antenna for on-body concealed weapons detections," *Piers Online*, Vol. 7, No. 5, 491–495, 2011.
9. Shafieha, J. H., J. Noorinia, and C. Ghobadi, "Probing the feed line parameters in Vivaldi notch antenna," *Progress In Electromagnetics Research B*, Vol. 1, 237–252, 2008.
10. Zhou, B., H. Li, X. Y. Zou, and T. J. Cui, "Broadband and high-gain planar Vivaldi antennas based on inhomogeneous anisotropic zero-index metamaterials," *Progress In Electromagnetics Research*, Vol. 120, 235–247, 2011.
11. Langley, J. D. S., P. S. Hall, and P. Newham, "Novel ultrawide-bandwidth Vivaldi antenna with low crosspolarisation," *Electron. Lett.*, Vol. 29, No. 23, 2004–2005, 1993.
12. Langley, J. D. S., P. S. Hall, and P. Newham, "Balanced antipodal Vivaldi antenna for wide bandwidth phased arrays," *IEE Proc. Microw. Antenna Propag.*, Vol. 143, No. 2, 97–102, Apr. 1996.
13. Gazit, E., "Improved design of the Vivaldi antenna," *IEE Proceeding*, Vol. 135, No. 2, 89–92, Apr. 1988.
14. Bai, J., S. Shi, and D. W. Prather, "Modified compact antipodal Vivaldi antenna for 4–50 GHz UWB application," *IEEE Trans. Microw. Theory Tech.*, Vol. 59, No. 4, 1051–1057, 2011.
15. Mehdipour, A., K. Mohammadpour-Aghdam, and R. Faraji-Dana, "Complete dispersion analysis of Vivaldi antenna for ultra wideband applications," *Progress In Electromagnetics Research*, Vol. 77, 85–96, 2007.

16. Yang, Y., Y. Wang, and A. E. Fathy, "Design of compact Vivaldi antenna arrays for UWB see through wall applications," *Progress In Electromagnetics Research*, Vol. 82, 401–418, 2008.
17. Hood, A. Z., T. Karacolak, and E. Topsakal, "A small antipodal Vivaldi antenna for ultrawide-band applications," *IEEE Antenna Wireless Propag. Lett.*, Vol. 7, 656–660, 2008.
18. Jolani, F., G. R. Dadashzadeh, M. Naser-Moghadasi, and A. M. Dadgarpour, "Design and optimization of compact balanced antipodal Vivaldi antenna," *Progress In Electromagnetics Research C*, Vol. 9, 183–192, 2009.
19. Fei, P., Y.-C. Jiao, W. Hu, and F.-S. Zhang, "A miniaturized antipodal Vivaldi antenna with improved radiation characteristics," *IEEE Antenna Wireless Propag. Lett.*, Vol. 10, 127–130, 2011.
20. Bourqui, J., M. Okoniewski, and E. C. Fear, "Balanced antipodal Vivaldi antenna with dielectric director for near-field microwave imaging," *IEEE Trans. Antennas Propag.*, Vol. 58, No. 7, 2318–2326, Jul. 2010.
21. Elsherbini, A., C. Zhang, S. Lin, et al., "UWB antipodal Vivaldi antennas with protruded dielectric rods for higher gain, symmetric patterns and minimal phase center variations," *IEEE Antennas Propag. Society International Symposium*, 1973–1976, 2006.
22. Kota, K. and L. Shafai, "Gain and radiation pattern enhancement of balanced antipodal Vivaldi antenna," *Electron. Lett.*, Vol. 47, 303–304, 2011.
23. Adamiuk, G., T. Zwick, and W. Wiesbeck, "Compact, dual-polarized UWB-antenna embedded in a dielectric," *IEEE Trans. Antennas Propag.*, Vol. 58, No. 2, 279–286, Feb. 2010.